Determination of resistivity response in carbonate rocks from Sergipe sub-basin

Marcus Vinícius Sousa Corrêa[1], Maria Rosilda Lopes de Carvalho[1], Rimary Valera Sifontes[1], Fernando Sérgio de Moraes[12], Victor Hugo Santos[12], †Carlos Alberto Dias[12]

[1]Grupo de Inferência de Reservatório - GIR/CCT/LENEP/UENF, [2]Instituto Nacional de Ciência e Tecnologia Geofísica do Petróleo - INCT-GP

Abstract

This theoretical-experimental study focuses on determining reservoir parameters such as porosity, permeability and saturation in carbonate rock samples from resistivity measurements. The objective is to develop correlations between the real and spectral resistivity domains. Based on the classical electrical model of Archie and its adaptations, this study also analyzes spectral induced polarization (SIP) data using Dias and Hybrid models. Analytical electrical models are proposed for the mechanism of electrolytic solution conduction in the pores of these rocks to understand their influence on electrical resistivity. The correlations between these models and the reservoir properties are established to apply and evaluate their sensitivity to the proposed electrical models and their integrations.

The results, presented in amplitude and phase curves of electrical resistivity, were fitted to the experimental data, allowing the estimation of the parameters for these models. The original Dias model could not satisfactorily fit the phase curves in the middle region of the spectrum. The hybrid model, on the other hand, provided a good fit in this region. Based on the parameters obtained with the Dias and hybrid models, permeability values were estimated by fitting the first phase peak associated with the ion diffusion process, where both models converged. The results showed values very close to those obtained from basic petrophysical measurements.

Introduction

Analysis of resistivity response in carbonate reservoirs is a major challenge for petrophysicists because porous media have complex transport properties characterized by complicated pore structures and surface properties (Fleury, 2002). Extensive research has been conducted on the analysis of water saturation in carbonate formations, which has yielded satisfactory results. However, the widely used Archie (1942) model is highly dependent on parameters such as pore geometry, connectivity, clay content, and other factors that strongly influence its accuracy. Therefore, detailed information on pore geometry is required to understand fluid displacement properties in carbonate deposits (Dixon & Marek, 1990), especially in cases where Archie's law fails due to challenges associated with understanding and predicting electrical resistivity based on microstructural effects at different pore scales. Researchers and industry professionals have developed analytical approaches to estimate water saturation and permeability to overcome these challenges while accounting for the excess conductivity created by clay volume or bound water and associated electrical properties. Winsauer & McCardell (1953) attributed the excess conductivity to an electrical double layer near charged clay surfaces resulting from surface adsorption and ion concentration. Building on these findings, Waxman-Smits (1968) developed a model that accounts for the cation exchange capacity of the clay to correct for variations in tone and volume. In addition, Clavier (1984) introduced the dual water model that distinguishes between water bound to clay and formation water to facilitate the necessary corrections. Similarly, Simandoux (1982) used clay volume and resistivity to account for the effects of clay minerals.

Induced electric polarization is another electrical behavior observed in rocks containing disseminated metallic and clay minerals. It occurs in response to the frequency of an applied electric field ranging from 1 mHz to 1 MHz. Numerous laboratory-scale studies have focused on establishing correlations between induced electric polarization parameters and the textural and hydraulic properties of rocks (Dias, 1968, 1972, 2000; Lima & Niwas, 2000; Barreto & Dias, 2014; Marinho & Dias, 2017; Marinho et al., 2018). These studies aim to estimate parameters related to the porous system and improve our understanding of their behavior in the subsurface (Tong & Tao, 2008; Revil et al., 2012; Barreto & Dias, 2014). Recent applications of the Dias model have shown favorable results in determining petrophysical parameters in siliciclastic samples (Marinho et al., 2018; Carvalho, 2019). In particular, the Hybrid model (Dias/Cole-Cole) is useful for accurately describing complex resistivities in an intermediate-range of the spectrum associated with heterogeneous medium. Therefore, there is great interest in further developing this method in carbonate rocks. To this end, we will discuss the models proposed by Dias (1968, 1972, 2000), who proposed an original electrical circuit models to describe the induced polarization (IP) effect observed in rocks. This model has been modified to include a "truncated" Cole-Cole impedance parallel with an ohmic resistor that forms a circuit in series with the Dias model.

Recent studies, such as those by Marinho (2018) and Carvalho (2019), have obtained satisfactory experimental results in siliciclastic samples. These studies have contributed to advances deriving petrophysical properties of porous media, especially permeability, using information obtained through SIP (spectrally induced polarization) model parameters. The model proposed by Dias and the Hybrid model have shown a strong correlation between experimental measurements and permeability estimates with a slight advantage for the Hybrid model. Thus, new relationships were established between the basic parameters of the model and the polarization mechanisms in rocks, linking the process of ion diffusion with hydraulic

permeability and allowing an approximate determination of this parameter.

Method

The rock samples studied were obtained from carbonate outcrops of the Sergipe Sub-Basin and consisted of 13 plugs. The experimental procedure with these samples was carried out at the petrophysics laboratory of LENEP-UENF in Macaé-RJ and included the following activities:

Geological characterization

Geological characterization of the samples includes data on mineral composition (%) by X-ray diffraction and fluorescence, using the Rietveld method (1969), and petrographic analysis of the samples to contextualize them in the geological framework. The objective was to identify the components responsible for the IP effect.

Basic Petrophysics

For basic petrophysical characterization of the samples, laboratory techniques are used to measure porosity (ϕ), permeability (k), and geometric parameters such as surface area and pore size distribution. Porosity will be measured using porosimetry techniques with an UltraPore-300 Helium Pycnometer System gas porosimeter following the API standard (1998). WINPORE software is used to calculate porosity based on the values of mass, diameter and length of sample plugs. The results include pore volume, grain volume, grain density and porosity fraction. The permeability of the sample plugs is measured using the Coreval-700 gas porosimeter from Vinci Technologies. This instrument provides high precision in determining permeability and porosity values in a single test. In addition, it can handle a variety of lithologies, including those with extremely high or low values for the petrophysical parameters measured.

Spectral Electrical Petrophysics

The acquisition of electrical petrophysical data involves the spectral measurement of the complex resistivity of samples, taking into account the induced polarization (IP) effect, in which the polarization mechanisms vary with frequency. Rock samples are saturated with a low-concentration electrolytic NaCl solution (0.01 M) prepared with deionized water ($\rho = 1.081 \times 10^4\ \Omega\mathrm{m}$) at 25°C. The saturation procedure is performed according to the instructions described by Worthington et al. (1990). Then, the saturated plug is placed in a sample holder with four non-polarizable, gold-coated silver electrodes that do not chemically react with the NaCl solution. The sample above holder is connected to the 1260 Impedance Analyzer instrument, where the variation of the complex electrical impedance is recorded in the frequency spectrum from 1 mHz to 100 kHz, at a constant temperature identical to that recorded during the porosity and permeability tests.

Modelagem dos Dados Experimentais

The complex electrical resistivity can be determined from the complex electrical impedance using the equation

$$\rho^* = \frac{Z^*}{g} = \rho' - i\rho'', \qquad (1)$$

where ρ^* is the complex electrical resistivity, Z^* is the complex electrical impedance, g is the geometric factor of the sample, i is the complex unit, and ρ' and ρ'' are the real and imaginary parts of electrical resistivity, respectively (Marinho & Dias, 2017). Once the values of ρ' and ρ'' are determined, the amplitude of the electrical resistivity (Ωm) and the phase (mRad) can be calculated for each frequency value using the following expression:

$$|\rho^*| = \sqrt{(\rho')^2 + (\rho'')^2}. \qquad (2)$$

After obtaining the amplitude and phase curves of resistivity for each sample, the experimental data were fitted with two electrical circuit models to describe the IP effect: first with the Dias model and then with a composite model. The fits for both models were determined by trial and error, with quality checked by the respective normalized root mean square error (NRMSE) values. Finally, permeability and average pore radius estimates were obtained from the Dias model parameters resulting from the modeling process.

Archie and Saturation Models

The Archie parameters are analyzed based on the log-log plot of the formation factor F against the porosity ϕ to determine the cementation coefficient ($\hat{m}$) and the proportionality parameter (a), which aims to model the relationship between the porous system and the degree of cementation using the linear regression given by:

$$\ln F = \ln a - \hat{m} \ln \phi \qquad (3)$$

Because the degree of cementation can affect the electrical measurements and thus the estimation of petrophysical properties, it is essential to understand the possible cementation and grain cohesion state of the samples.

The modified Simandoux equation, introduced by Bardon and Pied (1969), is commonly used to estimate water saturation in sandstones containing clay minerals.

$$\frac{1}{\rho_t} = \frac{{S_w}^2}{F\,\rho_w} + \frac{V_{sh} S_w}{\rho_{sh}} \qquad (4)$$

where V_{sh} is the volumetric fraction of clay in the rock, ρ_{sh} is the resistivity of the clay, S_w is the water saturation, and F is the formation factor given by the Archie equation. This equation represents an improved version of the original Simandoux equation that includes a quadratic component and accounts for the contribution of clay conductivity. This approach provides a more accurate representation of the complexity of rock systems, considering the parallel resistivities of the brine and clay components. Considering the clay mineral content, the modified Simandoux model is used to incorporate the Pickett cross-plot technique of rock resistivity and porosity, where the saturation curves account for the volume of clay minerals, to provide a detailed understanding of formation properties.

Dias model and Hybrid model

The Dias model used in modeling the experimental data is given by the original total current conductivity function proposed by Dias (1972, 2000, 1968) to describe the IP effect in rocks containing disseminated metallic minerals and/or clay minerals in contact with the electrolytic solution filling their porous spaces. This phenomenon has been studied since 1946 by several researchers in exploration geophysics. It has been observed in the frequency domain ranging from 1 mHz to 1 MHz under an applied harmonic electric field (time dependence $e^{i\omega t}$), and, correspondingly, in the time domain. The inverse function of the conductivity

of this model, represented byρ^* as a function of frequency $\omega = 2\pi f$, was redefined in terms of 5 primitive parameters $(\rho_0, m, \delta, \tau, \eta)$, as presented in Dias (2000).

$$\frac{\rho^* - \rho_\infty}{\rho_0} = \frac{m}{1 + i\omega\tau'\left(1 + \frac{1}{\mu}\right)} \quad (4)$$

where $i^2 = -1$, $\tau' = \left[\frac{1-\delta}{(1-m)\delta}\right]\tau$, $\mu = i\omega\tau\left[1 + \eta(i\omega)^{-\frac{1}{2}}\right]$ and $\rho_\infty = (1-m)\rho_0$. The terms ρ_0 and ρ_∞ are the values of ρ^* when$f \to 0$ and $f \to \infty$, respectively; m is the chargeability (dimensionless); τ is the relaxation time (s) with respect to the Helmholtz electric double-layer zone; η is the electrochemical parameter ($s^{-1/2}$); δ is the fraction of unit cell extension affected by the polarization effect due to the solid-liquid interface (Dias, 2000).

The term “Hybrid Dias/Cole-Cole model" refers to a model previously presented in works such as Marinho & Dias (2017) and Marinho et al. (2018), for simplicity, called here as Hybrid model. The main goal of this model is to improve data fitting in the intermediate frequency range, where the conventional Dias model is often inaccurate. To achieve this goal, the hybrid model is defined by the following approximate expression, which represents a frequency-dependent equation with:

$$\frac{\rho^* - \rho_\infty}{\rho_0} = \frac{m_{W1}}{1 + (i\omega\tau_{W1})^{\frac{1}{2}}} + \frac{m_{W2}}{1 + (i\omega\tau_{W2})^{c}} + \frac{m_D}{1 + i\omega\tau_D}, \quad (5)$$

The terms m_{W1}, m_{W2}, and m_D represent the partial chargeabilities associated with the low, intermediate, and high frequencies of the observed spectrum, respectively. These partial chargeabilities are related to the original chargeability of the Dias model (m) by the equation: $m = m_{W1} + m_{W2} + m_D$. Moreover, *Equation 5* depends on three different main relaxation times. According to Barreto & Dias (2014), τ_W and τ_D, which come from the original Dias model, are related to the ionic diffusion process within the electric double layer (at low frequencies) and the capacitive-resistive effect of this structure (at high frequencies), respectively. The term τ_{W2} represents the main relaxation time corresponding to a specific diffusion process affected by heterogeneities in each geological material. The parameter c characterizing the Cole-Cole functions (0 ≤ c ≤ 1) is related to the intensity of heterogeneities in the rock-fluid system.

Permeability Estimation from Dias Model Parameters

Revil & Florsch (2010) proposed a method for estimating permeability by relating the permeability coefficient (k) to the $\wedge$ term, based on previous work by Johnson et al. (1987), Avellaneda & Torquato (1991), Bernabé (1995), and Revil & Cathles III (1999). The expression for permeability is given as a function combining terms related to grain diameter and is defined as follows:

$$k = \frac{{d_g}^2}{32\hat{m}^2(F-1)^2F} \quad (6)$$

The determination of permeability k (mD) using parameters from the Dias model, obtained from modeled spectral electrical resistivity curves, was modified in *Equation 6* by replacing dg with $2l$ to estimate permeability in a porous medium (Barreto & Dias, 2014).

They also introduced the parameter η, which is a function of the thickness (l) of the electrical double layer and the cationic diffusion coefficient (D_c), expressed as follows:

$$k = \frac{D_c/\eta^2}{2\hat{m}^2(F-1)^2F \times 0{,}987 \times 10^{-15}} \quad (7)$$

This expression includes the diffusion coefficient of the electrolyte cation $D_c(m^2/s)$ (e.g..: Sodium $1.334 \times 10^{-9}\, m^2 s^{-1}$ @ 25 ºC (Bockris & Reddy, 2000)), the electrochemical parameter (η) specific to the Dias model, the cementation coefficient ($\hat{m}$), and the formation factor (F) from Archie's equation.

The permeability value is very sensitive to variations in the η parameter. It is interesting to note that the range of η curves from 0.1 to $10\, s^{-1/2}$ covers the permeo-porosity range commonly observed in experimental data of siliciclastic rocks. Higher η values indicate more extensive electrical double layers, suggesting that ions move over longer distances due to lower frequencies. This range probably encompasses the majority of cases of siliciclastic rocks. On the other hand, cases with values greater than $10\, s^{-1/2}$ correspond to rock samples with low permeability and high porosity.

Results

The rock samples were lithologically characterized as doloesparite, composed mainly of blocky dolomite, apparently replacing the original rock from a muddy matrix, due to the presence of intergranular residues and detrital grain volumes such as quartz, muscovite, biotite, and minerals with porous systems, including abundant vuggy pores, moldic pores likely resulting from the dissolution of bioclasts (due to their shape) or muddy intraclasts (due to clayey residues), and intercrystalline pores resulting from the dissolution of the matrix between dolomite crystals. As for the mineral phases identified by X-ray diffraction, the carbonates show a mineralogical diversity composed mainly of dolomite (80.25% to 97.45%) and calcite (0% to 2.57%). As for the occurrence of clay minerals, the diversity is greater, including illite (between 0.12% and 9.5%) and montmorillonite (between 0.07% and 0.54%). As for the basic petrophysical measurements, the analysis showed that the 13 carbonate samples have porosity values that fall within the range of moderate to good (15% - 20%) according to the classification of Levorsen (1967). The experimental permeability data showed considerable variation among the analyzed samples, ranging from good (10mD to 100mD). It is suggested that the significant dolomitization process in the rocks, which resulted in increased compactness due to increased cementation, may have contributed to a reduction in permeability.

The Archie parameters are analyzed using the log-log plot of the formation factor F against the porosity ϕ to determine the cementation coefficient ($\hat{m}$) and the proportionality parameter (a), which aims to model the relationship between the porous system and the degree of cementation. For 100% water-saturated samples, using linear regression, we obtain an average $\hat{m} = 1.81$ and $a = 0.49$. These values are within the reference range for carbonate rocks according to (Schon, 2011) and (Parkhomenco, 2012) and are consistent with the presence of fractures and weak cementation in the samples. In addition, a modified Pickett plot was used because the samples contain a small amount (2% on average) of clay minerals measured by X-ray diffraction (see *Figure 1*). As a result, saturation curves were estimated using the modified Simandoux model (Bardon & Pied, 1969), which

provided a more detailed understanding of formation properties such as permeability, porosity, and clay content. In addition to the above information, an empirical relationship was developed by Morris & Biggs (1967) to estimate relative permeability. This relationship involves the Archie equation and estimates the correlation of permeability zones with respect to irreducible water saturation, allowing the construction of parallel lines of constant permeability ranging from 0.01 to 100 mD.

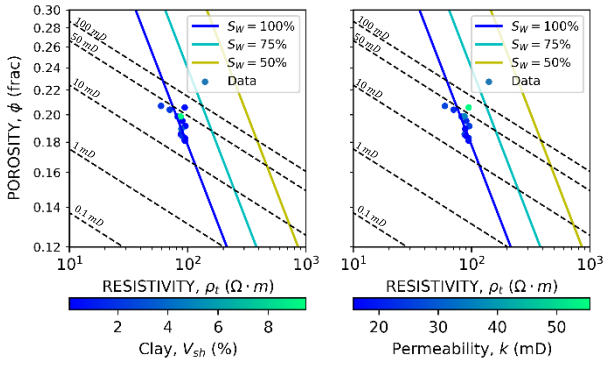

Figure 1: Curves of resistivity to rock porosity for different saturation values: 100%, 75% and 50%. Shows a) the clay content and b) the permeability of the sample.

In the modeling stage of the spectral electrical resistivity curves, the amplitude and phase curves of the experimental spectral electrical resistivity data in the frequency range from 1mHz to 100kHz for four samples are shown in *Figure 2*. The Dias and Hybrid models were used, incorporating the parameters obtained from fitting the experimental data listed in Table 1. The fitting of the experimental electrical resistivity data was performed using a trial-and-error procedure in which the quality of the fits for both amplitude and phase was evaluated for each connector individually using the Normalized Root Mean Square Error (NRMSE). The similarity of the curves results from similar petrophysical characteristics of the samples studied, extracted closely located points from the outcrop. The presence of two phase maxima can be observed. The first occurs at low frequencies and shows a slight tendency to occur in all measurements around the frequency of 1 Hz. According to Barreto and Dias (2014), this peak is associated with the anion-selective diffusion process of Na^+ ions from the electrolyte solution within the clay-electrolyte interface in the Helmholtz electrical double layer. The second maximum occurs at high frequencies and is related to the capacitive-inductive effect within the electrical double layer as a whole (Barreto & Dias, 2014). This latter maximum is more intense and does not reach completion at the frequency of 100kHz. In all samples, there is an extended and elevated phase plateau in the intermediate frequency range, around 101 Hz to 104 Hz. This is believed to be related to the differential diffusion process caused by the presence of heterogeneities such as microfractures, cracks, surface roughness of grains and pore walls combined with the complex geometry of clay minerals present in the samples. The IP effect is attributed to higher concentrations of illite clay minerals (between 0.12% and 9.5%) and lower concentrations of montmorillonite (between 0.07% and 0.54%).

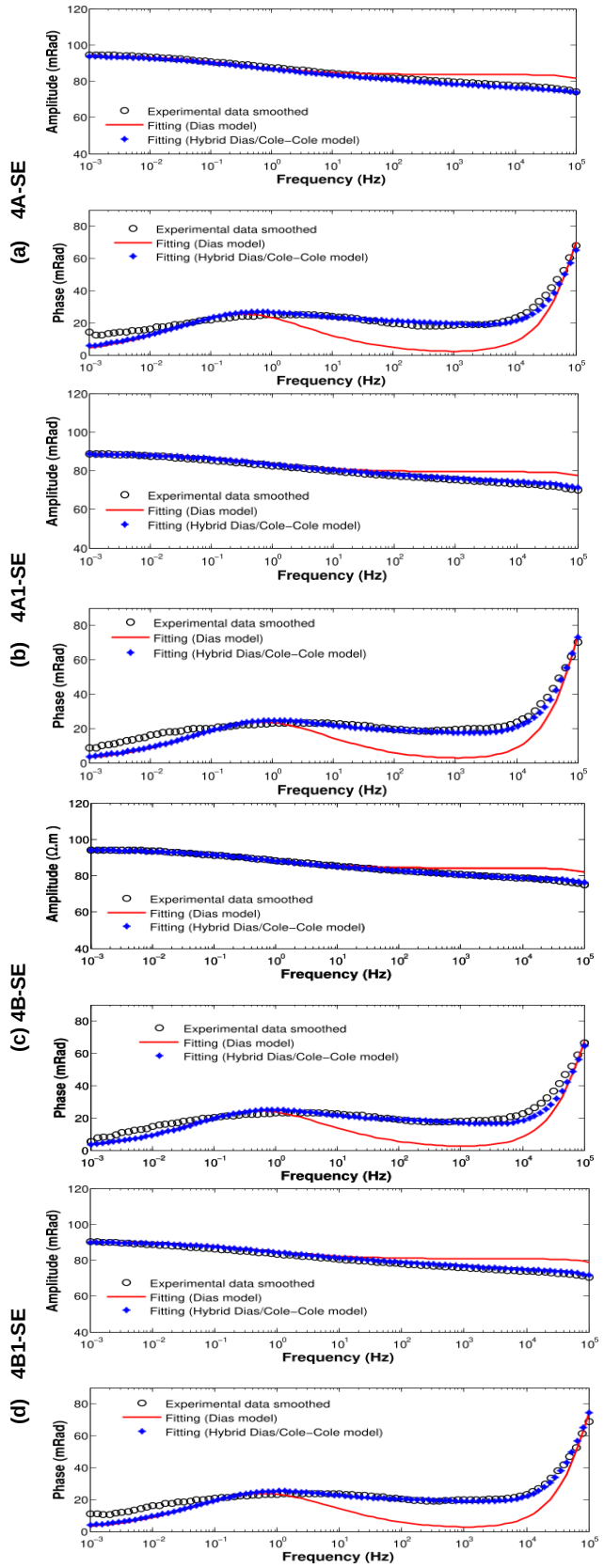

Figure 2: Experimental data and modeled amplitude and phase curves for samples (a) 4A-SE, (b) 4A1-SE, (c) 4B-SE and (d) 4B1-SE.

Table 1: Parameters of the Dias model and Hybrid model, obtained from the inversion procedure for samples 4A-SE, 4A1-SE, 4B-SE and 4B1-SE.

	Dias model	Hybrid Model (Dias/Cole-Cole)
4A-SE	original parameters $\rho_0 = 94.5\Omega m;$ $m = 0.29; \tau = 1.6 \times 10^{-6} s$ $\delta = 0.68; \eta = 2.2 s^{-1/2}$ derived parameters $\rho_0 = 94{,}5\Omega m;$ $m_W = 0{,}116; \tau_W = 0{,}571 s;$ $m_D = 0{,}174; \tau_D = 6{,}38 \times 10^{-7} s$ $f_a = 0{,}601; f_b = 0{,}399;$ $\nu = -3{,}5 \times 10^{-4}$ **Erro (NMRS):** $amp. = 0{,}038;\ fase = 0{,}462$	original parameters $\rho_0 = 94{,}5\Omega m;$ $m = 0{,}35; \tau = 1{,}65 \times 10^{-6} s$ $\delta = 0{,}66; \eta = 2{,}1 s^{-1/2};$ $m_{W2} = 0{,}15; \tau_{W2} = 9{,}4 \times 10^{-4} s;$ $c = 0{,}26$ derived parameters $\rho_0 = 94{,}5\Omega m; m_{W1} = 0{,}078;$ $m_{W2} = 0{,}15; m_D = 0{,}123$ $\tau_{W1} = 0{,}613 s; \tau_{W2} = 9{,}4 \times 10^{-4} s;$ $\tau_D = 6{,}5 \times 10^{-7} s; c = 0{,}26$ $f_a = 0{,}608; f_b = 0{,}392;$ $\nu = -3{,}3 \times 10^{-4}$ **Erro (NMRS):** $ampl. = 0{,}012;\ fase = 0{,}125$
4A1-SE	original parameters $\rho_0 = 94{,}5\Omega m;$ $m = 0{,}28; \tau = 1{,}6 \times 10^{-6} s$ $\delta = 0{,}68; \eta = 2{,}8 s^{-1/2}$ derived parameters $\rho_0 = 94{,}5\Omega m;$ $m_W = 0{,}111; \tau_W = 0{,}349 s;$ $m_D = 0{,}169; \tau_D = 6{,}32 \times 10^{-7} s$ $f_a = 0{,}605; f_b = 0{,}395;$ $\nu = -4{,}4 \times 10^{-4}$ **Erro (NMRS):** $amp. = 0{,}034;\ fase = 0{,}452$	original parameters $\rho_0 = 94{,}5\Omega m;$ $m = 0{,}323; \tau = 1{,}6 \times 10^{-6} s$ $\delta = 0{,}66; \eta = 2{,}7 s^{-1/2};$ $m_{W2} = 0{,}1; \tau_{W2} = 5{,}3 \times 10^{-4} s;$ $c = 0{,}33$ derived parameters $\rho_0 = 94{,}5\Omega m;\ m_{W1} = 0{,}089;$ $m_{W2} = 0{,}1; m_D = 0{,}134$ $\tau_{W1} = 0{,}379 s; \tau_{W2} = 5{,}3 \times 10^{-4} s;$ $\tau_D = 6{,}4 \times 10^{-7} s; c = 0{,}33$ $f_a = 0{,}601; f_b = 0{,}399;$ $\nu = -4{,}3 \times 10^{-4}$ **Erro (NMRS):** $amp. = 0{,}003;\ fase = 0{,}144$
4B-SE	original parameters $\rho_0 = 89\Omega m;$ $m = 0{,}31; \tau = 1{,}65 \times 10^{-6} s$ $\delta = 0{,}73; \eta = 2{,}9 s^{-1/2}$ derived parameters $\rho_0 = 89\Omega m;$ $m_W = 0{,}108; \tau_W = 0{,}281 s;$ $m_D = 0{,}202; \tau_D = 5{,}76 \times 10^{-7} s$ $f_a = 0{,}651; f_b = 0{,}349;$ $\nu = -3{,}8 \times 10^{-4}$ **Erro (NMRS):** $amp. = 0{,}043;\ fase = 0{,}456$	original parameters $\rho_0 = 89\Omega m;$ $m = 0{,}34; \tau = 1{,}86 \times 10^{-6} s$ $\delta = 0{,}69; \eta = 2{,}8 s^{-1/2};$ $m_{W2} = 0{,}12; \tau_{W2} = 4{,}0 \times 10^{-4} s;$ $c = 0{,}28$ derived parameters $\rho_0 = 89\Omega m; m_{W1} = 0{,}080;$ $m_{W2} = 0{,}12; m_D = 0{,}139$ $\tau_{W1} = 0{,}317 s; \tau_{W2} = 4{,}0 \times 10^{-4} s;$ $\tau_D = 6{,}8 \times 10^{-7} s;\ \ c = 0{,}28$ $f_a = 0{,}635;\ \ f_b = 0{,}365;$ $\nu = -4{,}2 \times 10^{-4}$ **Erro (NMRS):** $amp. = 0{,}008;\ fase = 0{,}142$
4B1-SE	original parameters $\rho_0 = 90{,}5\Omega m;$ $m = 0{,}31; \tau = 1{,}65 \times 10^{-6} s$ $\delta = 0{,}73; \eta = 2{,}8 s^{-1/2}$ derived parameters $\rho_0 = 90{,}5\Omega m;$ $m_W = 0{,}108; \tau_W = 0{,}301 s;$ $m_D = 0{,}202; \tau_D = 5{,}76 \times 10^{-7} s$ $f_a = 0{,}651; f_b = 0{,}349;$ $\nu = -3{,}7 \times 10^{-4}$ **Erro (NMRS):** $amp. = 0{,}050;\ fase = 0{,}464$	original parameters $\rho_0 = 90{,}5\Omega m;$ $m = 0{,}35; \tau = 1{,}86 \times 10^{-6} s$ $\delta = 0{,}69; \eta = 2{,}7 s^{-1/2};$ $m_{W2} = 0{,}13; \tau_{W2} = 4{,}0 \times 10^{-4} s;$ $c = 0{,}28$ derived parameters $\rho_0 = 90{,}5\Omega m; m_{W1} = 0{,}080;$ $m_{W2} = 0{,}13; m_D = 0{,}139$ $\tau_{W1} = 0{,}341 s; \tau_{W2} = 4{,}0 \times 10^{-4} s;$ $\tau_D = 6{,}8 \times 10^{-7} s;\ \ c = 0{,}28$ $f_a = 0{,}635;\ \ f_b = 0{,}365;$ $\nu = -4{,}1 \times 10^{-4}$ **Erro (NMRS):** $amp. = 0{,}012;\ fase = 0{,}132$

All samples show a broader and less pronounced low-frequency phase peak compared to the high-frequency peak, spanning about 4 decades of frequencies and values between 20 mRad and 25 mRad, while the high-frequency peak values range between 49.5 mRad and 72.7 mRad. The amplitude curves tend to approach asymptotes, with values ranging from 59.6 Ωm to 95.5 Ωm. The low intensity of the first phase peak is probably due to the low percentage of clay content, which is the cause of the IP effect. Lower clay content is believed to result in less coverage of the grains and pore walls by clay minerals in the samples, reducing the clay-electrolyte interface. This means a thinner Helmholtz electrical double layer and less diffusion within the double layer, reducing the intensity of polarization.

Despite the low expression of the low-frequency phase peak, a good fit was obtained with the Dias model for all samples, with average errors of 0.042 for the amplitude and 0.417 for the phase. However, despite the good fit of the two phase maxima obtained with the Dias model, as theoretically predicted by this model, it did not perform well in fitting the extensive and elevated phase plateau in the intermediate frequency region. Therefore, it was necessary to use the Hybrid model, which achieved an excellent fit of the phase curve in the intermediate frequency region, with average errors of 0.009 for amplitude and 0.145 for phase. When estimating the hydraulic permeability using the parameters of the Dias model, the first phase peak in the modeling phase must be accurately described. This is because the electrochemical parameter of the Dias model depends on the position of the phase peak associated with the ion diffusion process within the electrical double layer at low frequencies of the spectrum. Consequently, a good description of the first phase peak and its vicinity was obtained in the modeling of the experimental data of the electrical resistivity of the samples from the Sergipe sub-basin. This allowed the estimation of permeability by *Equation (7)* using the parameters of the Dias (k_{Dias}) and hybrid (k_{hyb}) models, respectively (see *Table 2)*. For samples that have estimated hydraulic permeability values with errors greater than 40% compared to the measured values, it is assumed that these discrepancies are due to a small instability observed in the phase curves at lower frequencies of the spectrum and poor resolution of the first phase peak. This complicates the accurate determination of the first phase peak, which directly affects the values of the parameters τ_{w1} and η, thus increasing the margin of error in the permeability estimation.

Table 2: Results of permeability estimates using parameters obtained from modeling of samples 4A-SE, 4A1-SE, 4B-SE, and 4B1-SE from the Sergipe Sub-basin.

Amostra	k_{exp} (mD)	*Permeabilidade* estimada (*k*) em mD			
		k_{Dias}	(ER%)	$k_{híb}$	(ER%)
4A-SE	55,59	46,46	(-16,41 %)	50,99	(-8,26 %)
4A1-SE	16,23	14,06	(13,35 %)	15,12	(-6,81 %)
4B-SE	16,79	16,35	(-2.57 %)	17,54	(4,51 %)
4B1-SE	15,66	14,99	(-4,31 %)	16,12	(2,91 %)

On the other hand, the remaining samples show estimated permeability values with errors below 17% compared to their respective laboratory-measured permeability values, indicating excellent results for both models used. The quality of the permeability estimates can be quantitatively assessed by applying the minimum residual logarithmic error (R), which is expressed as follows (Tong et al., 2006a).

$$[ln(R)]^2 = \frac{1}{N}\sum_{j=1}^{N}[ln\, k_M(j) - ln\, k_E(j)]^2, \qquad (8)$$

Compare the measured (k_M) and estimated (k_E) permeability values with the total number of measurements (N). Then $R = 1.32$ is obtained for the original Dias model

and $R = 1.18$ for the Dias/Cole-Cole hybrid model. These R values indicate how close the models are to the actual permeability measurements. A value of R close to 1 indicates that the model estimates permeability accurately, while larger values indicate less accurate estimates. In the present case, both the original Dias model and the Hybrid model performed well in estimating permeability compared to the measured values. This indicates that the models provide reliable and realistic estimates. It also highlights that the estimated permeability values of both models are generally very close. This means that the Hybrid model provides permeability estimates with the lowest errors compared to the original Dias model. These results indicate that both the original Dias model and the Hybrid model are effective in estimating permeability, but the hybrid model has an additional advantage in that it provides estimates with lower errors.

Conclusions

With a limited number of carbonate samples studied from the Sergipe sub-basin, the application of Archie's equation is also limited due to the diversity of pore types found in these samples. This diversity suggests that the samples have reasonable porosity but low permeability, reaching a maximum of 50 mD. This conclusion can be drawn based on the Archie parameters, with values of $a = 0.41$ and $\hat{m} = 1.81$ indicating that the rocks have become more compact due to the high degree of dolomitization caused by an increased amount of cement, resulting in lower permeability. Another factor affecting these parameters is the presence of clay minerals, which mainly affect the electrical behavior due to their distribution in the pore walls. X-ray diffraction analysis was used to identify the presence of clay minerals in the samples, mainly montmorillonite and illite, which have specific features on the grain surfaces. However, the cross-plotting resistivity and effective porosity technique proved useful in estimating fluid saturation and evaluating the distribution of clay minerals in the rocks studied. In addition, the permeability lines established are consistent with measurements made in the laboratory.

Spectral electrical resistivity measurements were of good quality for all samples in the frequency range from 1mHz to 100kHz. These measurements were represented by amplitude and phase curves. The amplitude curves showed no significant variation over the frequency range. The phase curves exhibited two peaks, indicating a broad and elevated plateau at intermediate frequencies, which is related to the textural and geometric heterogeneities of the porous medium. The experimental spectral electrical resistivity data were modeled using the original Dias and Hybrid model. The results, represented by amplitude and phase curves, were fitted to the experimental data to obtain the parameters of these models. The original Dias model does not adequately fit the phase curves in the intermediate region of the spectrum. However, the hybrid model provided a good fit in this region.

Based on the parameters of the Dias and the Hybrid model, permeability values were estimated by fitting the first phase peak associated with the ion diffusion process, where both models converged. The results yielded values very close or similar to those obtained from basic petrophysical measurements, despite a discrepancy in fitting the phase curves obtained from experimental electrical resistivity data to the phase curves obtained from modeling. The original Dias model had a minimum log residual squared error of R = 1.32, whereas the Hybrid model had R = 1.18.

Acknowledgments

We thank LENEP/UENF for the availability of the petrophysical laboratory and PETROBRAS for funding such infrastructure and this research. We also thank the technical support of the National Institute of Science and Technology - Petroleum Geophysics (INCT-GP).

References

Archie, G. E. (1942). The electrical resistivity log as an aid in determining some reservoir characteristics. *Transactions of the AIME*, *146*(01), 54-62.

Avellaneda, M., & Torquato, S. (1991). Rigorous link between fluid permeability, electrical conductivity, and relaxation times for transport in porous media. *Physics of Fluids A: Fluid Dynamics*, *3*(11), 2529-2540.

Bardon, C., & Pied, B. (1969, May). Formation water saturation in shaly sands. In *SPWLA 10th annual logging symposium*. OnePetro.

Bernabé, Y. (1995). The transport properties of networks of cracks and pores. *Journal of Geophysical Research: Solid Earth*, *100*(B3), 4231-4241.

Bockris, J. O. M., & Reddy, A. K. (2000). Electrochemistry in materials science. *Modern electrochemistry 2B: Electrodics in chemistry, engineering, biology, and environmental science*, 1637-1788.

Carvalho, M. R. L., 2019, Determinação de características petrofísicas de reservatórios através da medida espectral dos efeitos de polarização elétrica induzida em laboratório. 174 f. Tese (Doutorado em Engenharia de Reservatório e de Exploração) - LENEP / Universidade Estadual do Norte Fluminense Darcy Ribeiro.

Clavier, C., Coates, G., & Dumanoir, J. (1984). Theoretical and experimental bases for the dual-water model for interpretation of shaly sands. *Society of Petroleum Engineers Journal*, *24*(02), 153-168.

De Lima, O. A. L., & Niwas, S. (2000). Estimation of hydraulic parameters of shaly sandstone aquifers from geoelectrical measurements. *Journal of hydrology*, *235*(1-2), 12-26.

Dias, C. A. (1968). *A non-grounded method for measuring electrically induced polarization and conductivity*. University of California, Berkeley.

Dias, C. A. (1972). Analytical model for a polarizable medium at radio and lower frequencies. *Journal of Geophysical Research*, *77*(26), 4945-4956.

Dias, C. A. (2000). Developments in a model to describe low-frequency electrical polarization of rocks. *Geophysics*, *65*(2), 437-451.

Dixon, J. R., & Marek, B. F. (1990, September). The effect of bimodal-pore size distribution on electrical properties of some middle eastern limestones. In *SPE Annual Technical Conference and Exhibition*. OnePetro.

Fleury, M. (2002, September). Resistivity in carbonates: new insights. In *SPE annual technical conference and exhibition*. OnePetro.

Johnson, D. L., Koplik, J., & Dashen, R. (1987). Theory of dynamic permeability and tortuosity in fluid-saturated porous media. *Journal of fluid mechanics*, *176*, 379-402.

Levorsen, A. I., 1967, Geology of petroleum, 2d ed.. ed. [S.l.]: WH Freeman SanFrancisco.

Marinho, L. P., & Dias, C. A. (2017, August). Complex resistivity measurements on plugs from Corvina oil field, Campos basin, Brazil. In *15th International Congress of the Brazilian Geophysical Society & EXPOGEF, Rio de Janeiro, Brazil, 31 July-3 August 2017* (pp. 929-937). Brazilian Geophysical Society.

Morris, R. L., & Biggs, W. P. (1967, June). Using log-derived values of water saturation and porosity. In *SPWLA 8th Annual Logging Symposium*. OnePetro.

Nunes Barreto, A., & Alberto Dias, C. (2014). Fluid salinity, clay content, and permeability of rocks determined through complex resistivity partition fraction decomposition. *Geophysics*, *79*(5), D333-D347.

Parkhomenko, E. I. (2012). *Electrical properties of rocks*. Springer Science & Business Media.

Revil, A., & Cathles Iii, L. M. (1999). Permeability of shaly sands. *Water Resources Research*, *35*(3), 651-662.

Revil, A., & Florsch, N. (2010). Determination of permeability from spectral induced polarization in granular media. *Geophysical Journal International*, *181*(3), 1480-1498.

Revil, A. (2012). Spectral induced polarization of shaly sands: Influence of the electrical double layer. *Water Resources Research*, *48*(2).

Simandoux, P. (1982). Enhanced oil recovery: recent progress and trends. *Ind. Pet. Monde, Gaz-Chim.;(France)*, *50*(548).

Schön, J. (2011). *Physical properties of rocks: A workbook* (Vol. 8). Elsevier.

Tong, M., & Tao, H. (2008). Multi-exponential inversion of induced polarization relaxation signal of shaly sand. *Annals of Geophysics*.

Winsauer, W. O., & McCardell, W. M. (1953). Ionic double-layer conductivity in reservoir rock. *Journal of Petroleum Technology*, *5*(05), 129-134.

Waxman, M. H., & Smits, L. J. M. (1968). Electrical conductivities in oil-bearing shaly sands. *Society of Petroleum Engineers Journal*, *8*(02), 107-122.

Worthington A. E. P., Hedges J. H., PALLAT N., 1990a, SCA Guidelines for Sample Preparation and Porosity Measurement of Electrical Resistivity Samples, Part I: Guidelines for Preparation of Brine and Determination of Brine Resistivity for Use in Electrical Resistivity Measurements, The Log Analyst, 31, 20-28.